

Amplifier Similariton Fibre Laser with Nonlinear Spectral Compression

Sonia Boscolo⁽¹⁾, Sergei K. Turitsyn⁽¹⁾, Christophe Finot⁽²⁾

⁽¹⁾ Institute of Photonic Technologies, Aston University, Birmingham B4 7ET, United Kingdom

⁽²⁾ Laboratoire Interdisciplinaire Carnot de Bourgogne, UMR 6303, BP 47870, 21078 Dijon Cedex, France, christophe.finot@u-bourgogne.fr

Abstract We propose and numerically demonstrate a new concept of fibre laser architecture supporting self-similar pulse evolution in the amplifier and nonlinear pulse spectral compression in the passive fibre. The latter process is beneficial for improving the power efficiency as it prevents strong spectral filtering from being highly dissipative.

Introduction

Rapid recent progress in passively mode-locked fibre lasers is closely linked to new nonlinear regimes of pulse generation, namely, the self-similarly evolving, parabolic pulse (similariton)¹ and the all-normal-dispersion (dissipative soliton)² regimes. These are fundamentally different from the well-known soliton and dispersion-managed soliton regimes. More recently, similariton evolution in the gain segment of a fibre laser was demonstrated in a laser with an anomalous-dispersion segment³, in a Raman fibre laser and in an all-normal dispersion fibre laser⁴. In the latter configuration a narrow-band spectral filter provides the dominant mechanism for seeding the self-similar evolution in the amplifier by compensating both the broad pulse duration and bandwidth after the gain segment. The non-trivial interplay between the effects of gain, dispersion and nonlinearity in a fibre laser cavity leads to a variety of possible pulse shaping mechanisms not yet fully explored.

In this paper, we propose a new fibre laser design that takes advantage of the process of spectral compression arising from nonlinear pulse propagation in optical fibre⁵. We numerically demonstrate that both highly chirped amplifier similaritons and transform-limited picosecond pulses can be generated with the proposed scheme. Nonlinear spectral compression yields increased spectral brightness compared to direct spectral filtering.

Laser cavity architecture and numerical model

We consider a loop fibre laser configuration as shown in Fig. 1. A 3-m-long segment of ytterbium-doped fibre (YDF) with normal group-velocity dispersion (GVD) provides pulse amplification and supports similariton dynamics with nonlinear attraction. The gain fibre is followed by a saturable absorber (SA) element

and a large optical band-pass filter (OBPF) that enhances stability of the laser operation. After the filter, the pulse enters a dispersive delay line (DDL; realizable experimentally with a pair of diffraction gratings or a hollow core fibre) which provides anomalous GVD with negligible nonlinearity, and imparts a negative frequency chirp onto the positively (normally) chirped pulse as produced by the fibre amplifier. The negatively chirped, large-bandwidth pulse is then spectrally compressed in a 1.1-m-long segment of single-mode fibre with normal GVD (NDF: normally dispersive fibre). Indeed, for the negatively chirped pulse entering the fibre, where the long and the short wavelengths are in the trailing and leading edges, respectively, the effect of self-phase modulation is to redistribute both the long and the short wavelengths toward the center wavelength and therefore to spectrally compress the pulse instead of spectrally broadening it^{5,6}. This results in significant increase of the energy spectral density. Such spectral compression is the key feature of our laser set-up. A narrow OBPF is used after the NDF to suppress the spectral wings due to imperfect compression. Two output couplers are placed after the gain fibre and after the second OBPF, respectively.

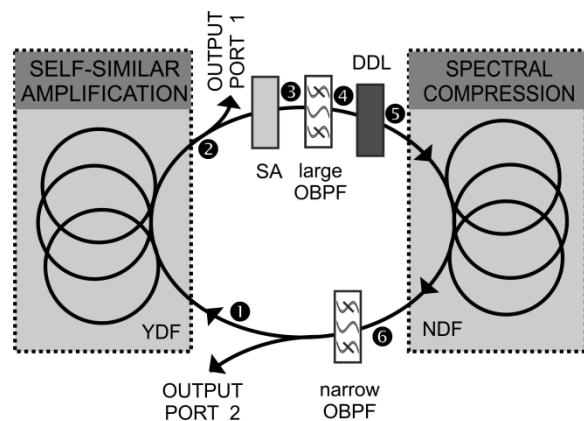


Fig. 1: Schematic of the laser.

Propagation within each section is modeled with a modified nonlinear Schrödinger equation for the slowly varying pulse envelope:

$$\frac{\partial \psi}{\partial z} = \frac{-i \beta_2}{2} \frac{\partial^2 \psi}{\partial t^2} + i \gamma |\psi|^2 \psi + \frac{g}{2} \psi \quad (1)$$

where β_2 is the GVD and γ is the coefficient of cubic nonlinearity for the fibre section, with $\beta_2 = 23 \text{ fs}^2/\text{mm}$ and $\gamma = 4.4 \cdot 10^{-3} \text{ /W/m}$ for the gain fibre, and $\beta_2 = 30 \text{ fs}^2/\text{mm}$ and $\gamma = 6.4 \cdot 10^{-3} \text{ /W/m}$ for the NDF. g is the net gain, which is non-zero only for the gain fibre. The gain saturates with total energy according to $g = g_0 / (1 + W/W_0)$, where $g_0 = 30 \text{ dB/m}$ is the small-signal gain with an implicit parabolic frequency dependence and a bandwidth of 40 nm, $W(z) = \int dt |\psi|^2$ is the pulse energy, and $W_0 = 250 \text{ pJ}$ is the gain saturation energy determined by the pump power. The SA is modeled by a transfer function that describes its (monotonic) transmittance, $T(t) = 1 - q_0 / [1 + P(t)/P_0]$, where $q_0 = 0.8$ is the unsaturated loss, $P(z, t) = |\psi(z, t)|^2$ is the instantaneous pulse power, and $P_0 = 200 \text{ W}$ is the saturation power. The OBPFs are Gaussian transfer functions with 5-THz and 0.5-THz full-width at half-maximum (FWHM) bandwidth, respectively. The DDL provides a total dispersion of -119 fs^2 . A linear loss of 60% is imposed at each output port. The numerical model is solved with the standard split-step Fourier method and the initial field is white noise. The simulations are run until stable operation of the laser is obtained after a finite number of round trips in the cavity.

Pulse shaping in the cavity

The steady-state intra-cavity pulse dynamics is illustrated by plots of the temporal and spectral pulse evolutions (Fig. 2), and of the evolutions of the root-mean-square (rms) pulse duration and spectral bandwidth (Fig. 3) over one round-trip. Also shown (Fig. 2) is the intra-cavity dynamics that occurs in a standard amplifier similariton fibre laser consisting of an YDF segment, a SA and an OBPF⁴. The FWHM bandwidth of the filter is 2 THz for the standard cavity, which is the minimum value permitting stable laser

operation, while other system parameters are the same as those mentioned in the previous section. The pulse solution at different positions in the cavity is shown in Fig. 4. The pulse duration and bandwidth increase monotonically in the gain fibre as the pulse evolves towards the asymptotic attracting solution in the fibre (Figs. 2, 3), consistently with what is well known from self-similar propagation⁷ and mode-locking. A typical feature of amplifier similaritons is indeed that the pulses evolve toward a parabolic asymptotic solution⁷: the pulse is nearly parabolic in shape at the end of the gain fibre (Fig. 4a). The associated spectrum exhibits some structure, as expected for a parabola with finite (though large) chirp. This pulse has a time-bandwidth product (TBP) of approximately 17. Cancellation of the rather highly linear chirp outside the cavity can lead to high-quality temporally compressed pulses with durations as short as 100 fs and peak powers well above 10 kW.

In the standard similariton laser, the spectral filter compensates both the broad pulse duration and bandwidth after the gain segment (Fig. 2b). Thus, the main pulse shaping mechanism relies on the attracting nature of amplifier similaritons, which is then compensated by strong spectral filtering. However, such filtering introduces high energy loss. In contrast, the pulse shaping mechanism of the laser design proposed in this paper is dominated by two distinctly different nonlinear processes: similariton formation with nonlinear attraction in the gain fibre, and spectral compression arising from nonlinear propagation in the passive fibre and leading to large spectral narrowing (Fig. 3). The first OBPF carves the output spectrum from the amplifier, and the linear DDL only affects the temporal width of the pulse. It is worth noting that this pulse dynamics is fundamentally different from that of a fibre cavity with a dispersion map. The spectral compression factor, which is defined as the ratio of the FWHM widths at the input and output of the passive fibre, is approximately 6

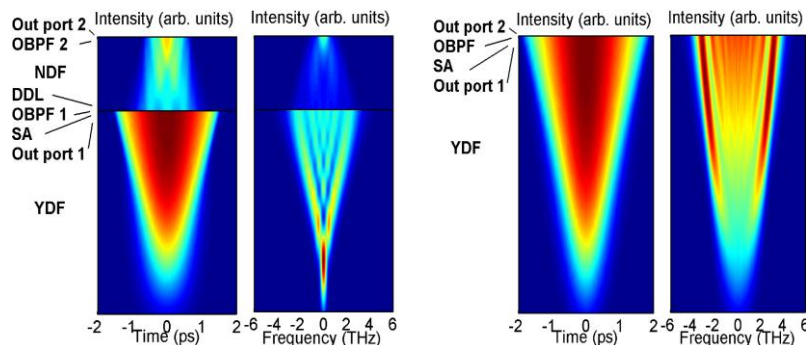


Fig. 2: Evolution of the temporal (left) and spectral (right) intensity profile of the pulse in the cavity (a) with and (b) without nonlinear spectral compression.

and corresponds to an output FWHM width of 0.8 THz (Fig. 4b). The latter is comparable to the bandwidth of the narrow OBPF. The energy spectral density of the pulse is therefore largely increased, and nonlinear spectral compression prevents strong spectral filtering from being highly dissipative. The output pulse from the passive fibre exhibits a nearly transform-limited picosecond profile with a TBP nearly equalizing the transform limit for a Gaussian pulse (0.441). Note that the direct generation of transform-limited picosecond pulses is very difficult to achieve in conventional laser cavities supporting self-similar evolution in active or passive NDF.

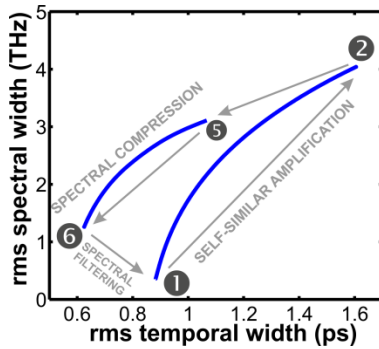


Fig. 3: Phase diagram representing the combined evolution of the temporal and spectral rms widths of the pulse over one round-trip. The locations in the cavity indicated in Fig. 1 are shown.

Conclusions

We have numerically investigated a fibre laser design whose pulse shaping mechanism relies on similariton formation with nonlinear attraction in the gain segment of the oscillator and nonlinear spectral compression in the passive fibre. We have shown that nonlinear spectral compression is beneficial for improving the energy efficiency of the cavity as it prevents strong spectral filtering from being highly dissipative. Larger compression factors or output pulse energies can be obtained by further scaling of the cavity parameters.

Acknowledgements

The authors would like to acknowledge support from the Leverhulme Trust (grant RPG-278), the British Council (Alliance grant 10.002), the

Région Bourgogne (PARI PHOTCOM), and the Ministère des Affaires étrangères et européenne (Alliance grant 22836ZJ).

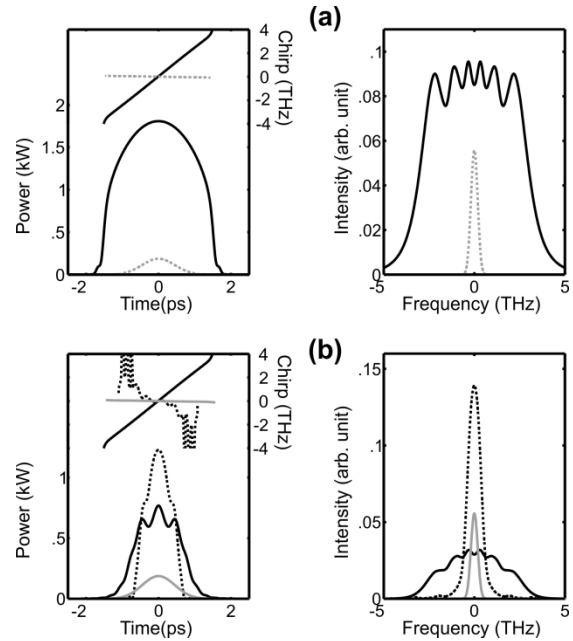


Fig. 4: Temporal intensity and chirp profiles (left) and spectral intensity profiles (right) of the pulse at (a) the entrance (location ❶ in Fig. 1; dotted curves) and the exit (location ❷ in Fig. 1; solid curves) of the gain fibre, and (b) the entrance of the passive fibre (location ❸ in Fig. 1; solid black curves), the end of the passive fibre (location ❹ in Fig. 1; dotted black curves), and after the narrow spectral filter and output coupler (location ❶ in Fig.1; solid gray curves).

References

- [1] F.Ö. Ilday et al., Phys. Rev. Lett. **92**, 213902 (2004).
- [2] F.W. Wise et al., Laser & Photon. Rev. **2**, 58 (2008).
- [3] B. Oktem et al., Nat. Photon. **4**, 307 (2010).
- [4] W.H. Renninger et al., Phys. Rev. A **82**, 021805(R) (2010).
- [5] S.A. Planas et al., Opt. Lett. **18**, 699 (1993).
- [6] E.R. Andresen et al., Opt. Lett. **36**, 707 (2011).
- [7] M.E. Fermannet et al., Phys. Rev. Lett. **84**, 6010 (2000).